Analysis of a software-based A-GPS acquisition performance using statistical processes

Damien Kubrak, Christophe Macabiau, Michel Monnerat

Analysis of a software-based A-GPS acquisition performance using statistical processes

Damien Kubrak, *Ecole Nationale de l'Aviation Civile / TéSA*, France
Christophe Macabiau, *Ecole Nationale de l'Aviation Civile*, France
Michel Monnerat, *Alcatel Space*, France

BIOGRAPHY

Damien Kubrak is a Ph.D. student in the field of personal positioning in the signal processing lab of the Ecole Nationale de l'Aviation Civile (ENAC) in Toulouse, France. He graduated in 2002 as an electronics engineer from the ENAC, and received the same year his Master research degree in signal processing.

Christophe Macabiau graduated as an electronics engineer in 1992 from the ENAC (Ecole Nationale de l'Aviation Civile) in Toulouse, France. Since 1994, he has been working on the application of satellite navigation techniques to civil aviation. He received his Ph.D. in 1997 and has been in charge of the signal processing lab of the ENAC since 2000.

Michel Monnerat graduated from the ENSICA (Ecole Nationale Supérieure d'Ingénieur de Constructions Aéronautiques) engineering school. After being involved within Alcatel Space in many radar programs, in charge of the onboard processing of the ARGOS / SARSAT payload, he has been involved in the Galileo program since 1998, for the signal design and performance aspects.

ABSTRACT

The efforts of the semiconductor industry to produce small, low consumption and powerful chipsets bear fruit, and many portable devices are now equipped with them. Indeed, the miniaturized chipsets with increasing processing power make them suitable for supporting software-based applications. On the other hand, demand for indoor navigation and location based services applications, whose interoperability with GNSS technology is being more and more obvious, is expected to grow rapidly in the next few years. In this context, because of their maximum flexibility and minimum hardware modifications, software-based positioning techniques embedded in portable devices become very interesting. The remaining key point is the time needed to acquire these rare and weak indoor signals and give a position solution.

The aim of this study is to present results on the time needed to acquire one satellite for such embedded GPS applications, and more specifically, for Assisted-GPS ones. In this paper, an RF front-end chipset combined with a processor embedded in a portable device is considered. Only the acquisition process using FFT correlations will be studied here.

The classical structure for L1 code FFT acquisition is first described and acquisition performance, such as the mean acquisition time, is discussed. A statistical process is used to simulate acquisition procedures, according to probabilities of detection, acquisition structure and the implemented acquisition strategy. The estimated times are then deduced from these tests. A special study is carried out to measure the impact of the Doppler affecting the GPS signal. An analysis of the effect of the computational power is also conducted, as well as the influence of the signal-to-noise ratio on the acquisition procedure, mostly dedicated to indoor and deep indoor environments.

Results point out the fact that to achieve the requirements of the application supporting the software-based acquisition process, a trade-off has to be found between performance relative to the acquisition of weak signals, and the rapidity of the processing, especially in deep indoor environments. The evaluation of the Doppler component due to user dynamics and the acquisition strategy are also key points that would speed up the process.

INTRODUCTION

The Location based services are taking more and more emphasis for telecommunication applications. Our society is indeed being influenced by the emerging mobility culture driven by the development of new technologies. In parallel to this growing demand, regulation aspects played and still play a role of key driver : E911 regulation for North America and E112 in Europe. The aim of such regulations was to force the mobile operators to locate any distress call with a certain level of accuracy and availability – 50m for 68% of the calls and 100m for 95% of them for E911, European operators "best effort"

performance for E112. Among several location techniques, Assisted GPS seems to emerge as a very promising one. The reasons for this are the location accuracy provided by the Assisted GPS, much better than other techniques (Cell, ID, EOTD, TOA etc…), and compliant with the E911 requirements.

The assistance technique aims at combining a cellular phone with a Global Navigation Satellite System (GNSS) receiver. The principle of such techniques is described in [Digge01]. The different elements involved are a mobile phone able to process GPS signals, a cellular network and an assistance data server. To provide a position estimate, the mobile is able to require assistance data from the dedicated server through the cellular network :

Reference location	Pre location of the mobile generally deduced from cellular information.
Reference time	GPS time reference.
Navigation model	Visible satellites ephemeris and clock corrections.
Ionosphere corrections	Klobuchar model parameters broadcast by the GPS satellites.
Differential correction	Standard differential corrections.
Real time integrity	List of bad satellites.
Almanacs	Almanacs of the GPS constellation.
UTC model	UTC model parameters broadcast by the Signal in space.
Acquisition assistance	List of assistance to improve the acquisition.

Table 1 – Assistance data

This data provides information that is used to first improve the sensitivity of a GNSS receiver and then decrease the time needed to fix. Because of the reduction of the overall computational cost, A-GPS positioning technique is thus well suited to be implemented in software embedded in a mobile phone. However, given the fact that the user is likely to evolve outdoors as well as indoors, the C/N_0 ratios of signals to acquire are widely spread from the typical outdoor one to the weakest indoor one. Consequently, it impacts the performance of the receiver in terms of acquisition time.

In this paper, an analysis of the performance of such typical embedded A-GPS software dedicated to personal positioning is addressed. Since the user is likely to require its position in indoor environments, C/N_0s of the signals to acquire will be weak. Therefore, to avoid false alarms that would lead to a bad position solution, a precise positioning performed by an accurate assisted acquisition process using FFT correlations will be considered in the following. The assistance message is supposed to be provided through the GSM non synchronous cellular network.

In the next section, the classical FFT acquisition structure used for simulations is presented, as well as its principle. Assisted GPS improvements are then highlighted in section 2. Section 3 provides results of the simulations processed to characterize the time needed to successfully acquire signals of different power.

I – ACQUISITION SCHEME

a) Analytical signal expression

The structure of the accurate acquisition process is presented in Figure 1. It is composed of three main parts :

1. the RF front-end
2. the base-band transformation
3. the acquisition loop

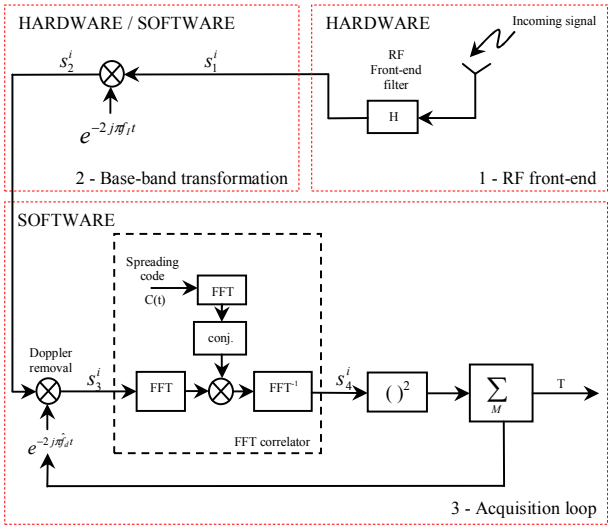

Figure 1 – L1 Acquisition structure.

In order to analyse the performance of such a software-based assisted acquisition structure, expressions of the signal at different stages are derivated. The incoming RF L_1 signal s_0^i from GPS satellite i at the antenna output has the following expression :

$$s_0^i(t) = Ad^i(t-\tau^i)c^i(t-\tau^i)\Re e\left\{e^{j\cdot\left(2\pi f_{L_1}(t-\tau^i)+\phi^i\right)}\right\} + n_0^i(t)$$

where :

- A is the amplitude of the signal.
- d^i is the GPS navigation message.
- τ^i is the propagation delay.
- c^i is the Gold spreading code.
- ϕ^i is the residual phase to the origin.

- f_{L_1} is the GPS L_1 frequency.
- n_0^i is the centred white Gaussian noise, with a $N_0/2$ PSD.
- $\Re e$ is the real part of the complex expression.

The signal next enters the RF front-end to be filtered through the RF front-end filter H of bandwidth B Hz, and converts the L_1 frequency down to the intermediate frequency f_I. At the output of the RF front-end filter, the signal is modelled as follows :

$$s_1^i(t) = Ad^i(t-\tau^i)c_f^i(t-\tau^i)\Re e\left\{e^{j\cdot\left(2\pi f_{L_1}(t-\tau^i)+\phi^i\right)}\right\} + n_1^i(t)$$

where :

- c_f^i is the filtered spreading Gold code.

The next stage is the base-band reduction of the incoming signal, by multiplying s_1^i with an imaginary exponential such that the real part of the resulting complex signal is the in-phase one of the classical structure, and the imaginary part the quadrature one. Since the acquisition loop FFT correlator acts as a low-pass filter, the high frequency terms are cut off. Therefore, the useful complex baseband signal s_2^i can be written as :

$$s_2^i(t) = \frac{A}{2}d^i(t-\tau^i)c_f^i(t-\tau^i)e^{j\left[2\pi f_d^i(t)\cdot t+\psi^i\right]} + n_2^i(t)$$

where :

- $\psi^i = \phi^i +$ non-linear terms over time.
- f_d^i is the actual Doppler frequency affecting the signal from satellite i.

The signal then enters the acquisition loop where the classical two dimensional delay/frequency search is performed. The first step of the FFT acquisition procedure is to remove the Doppler affecting the received signal by sweeping over the whole Doppler range ($\pm$ 6kHz). At this stage, the signal is given by :

$$s_3^i(t) = \frac{A}{2}d^i(t-\tau^i)c_f^i(t-\tau^i)e^{j\left[2\pi\Delta f_d^i\cdot t+\psi^i\right]} + n_3^i(t)$$

where :

- $\Delta f_d^i = f_d^i - \hat{f}_d^i$ is the difference between the actual and the estimated Doppler.
- $\hat{f}_d^i$ is the estimated Doppler frequency.

The signal is then correlated in the FFT correlator with a local replica of the spreading code corresponding to the PRN to acquire, in order to detect the propagation delay affecting the received signal. The code Doppler is at this stage taken into account. Assuming that the length of the signal used to compute Fourier transformations, i.e. the coherent integration time, is equal to T_p seconds, and also that there is no bit transition occurring during the integration, the signal at the entrance of the multiplier in the FFT correlator is as follows :

$$s_4^i(t) = \frac{A}{2}e^{j\psi^i}d_{T_p}^i \cdot FT\left[rect_{T_p}\cdot c_f^i(u-\tau)\cdot c^i(u)\right]_{f=-\Delta f_d^i} + n_4^i(t)$$

where :

- $d_{T_p}^i$ is the data bit value over the T_p seconds.
- $rect_{T_p}$ is the rectangular function centred in $T_p/2$.
- $t \in [0, T_p]$.

A straightforward calculation leads to the following expression of the Fourier transform :

$$FT\left[rect_{T_p}\cdot c_f^i(u-\tau)\cdot c^i(u)\right]_{f=-\Delta f_d^i} = S_c(f) * S_{c_f}(f)e^{-2j\pi f\tau} * T_p e^{-j\pi f T_p}\left.\frac{\sin(\pi f T_p)}{\pi f T_p}\right|_{f=-\Delta f_d^i}$$

where :

- S_c is the Fourier transform of the local replica of the spreading code c
- S_{c_f} is the Fourier transform of the filtered incoming spreading code c.

Moreover, assuming the spreading code is T_R-periodic and is also materialized by the waveform m, its Fourier transform is given by :

$$S_c(f) = f_R\sum_{u\in Z} C(u)M(uf_R)\delta(f-uf_R)$$

where :

- C is the Fourier transform of the digital version of the spreading code c.
- M is the Fourier transform of the waveform m.

– $f_R = 1/T_R$.

Consequently, assuming negligible the effect of the RF front-end filter – i.e. $S_{c_f}(f) \approx S_c(f)$ – and no bit transition during the coherent integration, the signal at the output of the FFT correlator is finally given by :

$$s_4^i(t) = \frac{AT_p d^i_{T_p}}{2} \cdot \frac{\sin\left(\pi \Delta f_d^i \cdot T_p\right)}{\pi \Delta f_d^i \cdot T_p} \cdot K_c(t) \cdot e^{j\left(\pi \Delta f_d^i \cdot T_p + \psi^i\right)} + n_4^i(t)$$

where :

– K_c is the autocorrelation of the spreading code c .

Since n_4^i is assumed to follow a normal distribution with zero mean, its variance can be expressed as :

$$\sigma^2_{n_4^i} = E\left[\left(\int_{u=0}^{T_p} n_1^i(u) \cdot c(u) \cdot e^{-j2\pi\left(f_I + \hat{f}_d^i\right)u} \cdot du\right)^2\right]$$

The RF front-end filtering effect being neglected, that is $E\left[n_1^i(u) \cdot n_1^i(v)\right] = \frac{N_0}{2}\delta(u-v)$, the variance of the noise is finally given by :

$$\sigma^2_{n_4^i} = \frac{N_0}{2f_p}$$

where :

– $f_p = 1/T_p$.

b) Acquisition principle

Once the signal has been correlated in the FFT correlator, it is squared, the magnitude is computed and stored into memory. Then, another T_p seconds of base-band signal enters the acquisition loop, is processed through the FFT correlator, squared and added to the previous result. It is then repeated M times, M being the non-coherent integration number, for each Doppler bin such that the result of the processing is the criterion T matrix.

The criterion T is a matrix whose columns are the delay bins and the rows the Doppler bins. As a consequence, each row contains the squared autocorrelation vector K_c over the T_p seconds, weighted by the Doppler interference term $\frac{\sin\left(\pi \Delta f_d^i \cdot T_p\right)}{\pi \Delta f_d^i \cdot T_p}$.

Since the shape of the autocorrelation K_c is a triangle of width 2 chips, if the noise power is reduced enough and the difference between the actual and the estimated Doppler small enough, the detection of the autocorrelation peak is possible, as it is illustrated in Figure 2.

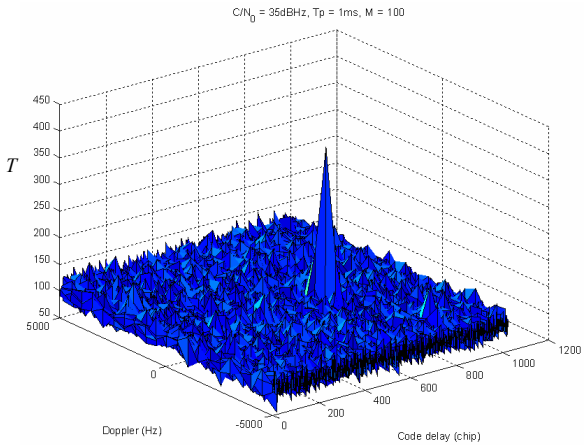

Figure 2 – Acquisition Loop output T .

The criterion computation is performed over the whole frequency uncertainty affecting the incoming signal ($\pm$ 6kHz), as well as the whole propagation delay uncertainty (1ms). In the next section, their reduction thanks to assistance data are discussed, especially those of the frequency since FFT operations compute at once the correlation over the coherent integration time.

II – A-GPS IMPROVEMENTS

The assistance message provides some information that is useful to reduce the Doppler uncertainty region. On one hand, the ephemeris data are likely to provide an estimate of the position of the satellites, according to the algorithm presented in [Navst95]. On the other hand, a rough location of the user requesting assistance is also provided through the assistance message. Therefore, given two successive positions of one satellite, and assuming a static user, it is then possible to predict the contribution of the satellite of interest on the overall Doppler. As a consequence, the Doppler uncertainty region is dramatically reduced.

If the GPS time and the user position transmitted in the assistance message were exact, the estimation of the Doppler shift between the user and GPS satellite in visibility would be accurate. But because of the uncertainty on user's position (35 km, which is the maximum GSM cell size) and GPS time ($\pm$ 2s, provided

through the GSM non synchronous cellular network), this Doppler estimation is also computed with some uncertainty.

Figure 3 shows the Doppler uncertainty in the worst case caused by a GPS time error of ± 2s in the Doppler computation algorithm presented in [Navst95]. The data used to simulate the assistance message are the one contained in the YUMA almanacs for PRN1 collected on Tuesday, January 04th, 2005 3:29 PM (downloaded from the US Coast Guard website). No uncertainty on the user's position was considered in this test. The user is assumed to be static and its position is equal to that of the reference GPS antenna at the signal processing lab at the ENAC.

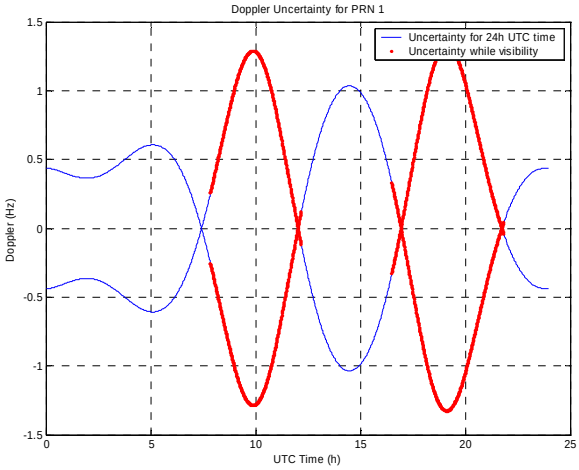

Figure 3 – Doppler uncertainty, GPS time at +/- 2s.

From the envelope plotted in Figure 3, it appears that the uncertainty in time does not impact the estimation of the satellite Doppler. Indeed, the error on the predicted Doppler is at worst 1,25 Hz. And this result goes for all PRNs. On the other hand, standardization of the assistance message through the GSM network tends to make possible the transmission of precise GPS time. Consequently, the uncertainty on the overall Doppler brought by GPS time uncertainty can be considered not to be an issue anymore on the Doppler estimation.

However, as it has been discussed in the previous section, the user initial position is located inside the area covered by the Base Transceiver Station the cell-phone depends on, which means that the true position of the user is those of the BTS, plus an undetermined distance from the BTS antenna to the mobile. This distance can not be longer than 35 km, because of the design of the GSM cells.

Figure 4 shows the Doppler uncertainty involved for a GSM cell size of 35 km, assuming a static user. Satellite number 1 is taken into account for week number 280, as in the previous case. Moreover, the ambiguity on the user's position is applied in the local frame along the north axis. Under these assumptions, the maximum uncertainty on the estimation of the satellite Doppler contribution is about ± 30Hz.

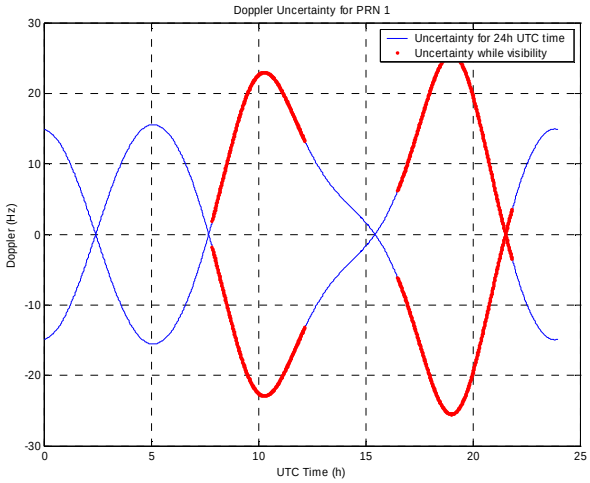

Figure 4 – Doppler uncertainty, cell of 35 km radius.

For typical GPS signals reception, the total frequency uncertainty is approximately 12 kHz and depends mainly on three factors : the satellite Doppler contribution – about ± 4 kHz, the local oscillator drift – a typical 1 ppm accurate local oscillator induces a ± 1.5 kHz uncertainty, and the user Doppler contribution – up to ± 200 Hz (for a typical in-vehicle user motion). Assuming the local oscillator drift compensated, and given the former results, the total uncertainty affecting the frequency of the received signals lies within the range of ± 230 Hz. Compared with the ± 6 kHz in the non assisted mode, the improvement is obvious. On the other hand, assistance data provide means to reduce the time range as well. Therefore, the A-GPS acquisition is processed over a reduced area, as presented Figure 5.

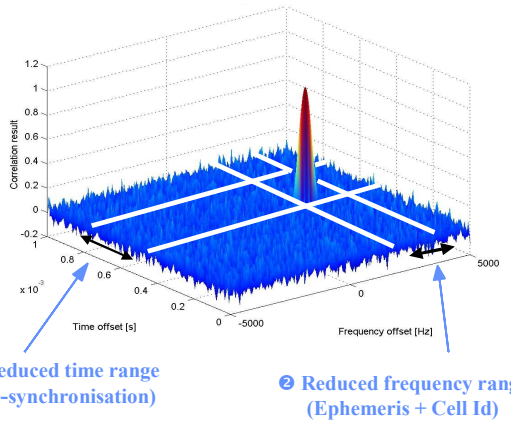

Figure 5 – A-GPS improvements.

Given these improvements, the receiver could then

concentrate its computation capability on increasing the sensitivity (i.e. acquiring weak signals) or equivalently the time to fix. Indeed, as presented in Table 2, the acquisition complexity is well reduced in the assisted mode, enabling weak signals correlation peak detection using large coherent integration times. Whatever the coherent integration time, the acquisition complexity improvement is well above +1000% for the A-GPS mode, compared with the GPS one.

Coherent integration		1ms	10ms	20ms
Total bins number	GPS	49104	472626	943206
	A-GPS	4092	26598	51150
Comparison GPS relative to A-GPS (%)		+1200	+1777	+1844

Table 2 – Acquisition complexity comparison.

A tradeoff has clearly to be found between the capability of acquiring weak signals, and the time elapsed to compute a position. It is discussed in the next section.

III – ACQUISITION METHODOLOGY

The global positioning technique leading to the computation of a position and implementing the acquisition loop is presented Figure 6.

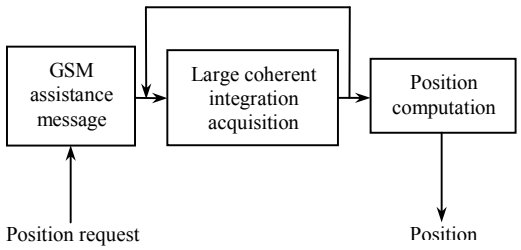

Figure 6 – Positioning technique basics.

Basically, since the receiver is to be used indoors, weak signals are likely to be acquired. Therefore, a large coherent integration time shall be taken in order to greatly reduce the power of the noise. In the best case, the bit transition is known and the receiver can trigger a 20ms coherent integration. If not, various techniques can be used to allow large coherent integration, such as bit transition detection. The process repeats at least three more times to acquire four satellites and then a fix is computed.

One big issue involved in our application is that weak signal makes it very difficult for possible tracking loops to check if the detected peak is the true correlation one. To avoid this issue, a false alarm probability shall be chosen consequently, depending on the number of bins to be tested in the detection process. For instance, if the sampling frequency is twice the chips rate, 2046 hypotheses have to be tested. Doppler bins have to be taken into account as well (typically 3 in a static mode, whatever the coherent integration time, because of the assistance message Doppler uncertainty reduction). Since there are nearly 6000 cells to test, a probability of false alarm of 10^{-5} meets the requirement of detecting almost all the time a true correlation peak. Several tests were conducted to assess 10^{-5} was a good compromise between the time needed to acquire a satellite, and the successful detection of a correlation peak.

The time needed to acquire one satellite, with respect to its C/N_0 can then be estimated. This time is divided into two parts, the first one being the useful signal duration (or required signal duration), the second one the processing time leading to the success of the acquisition. The processing time is related to the performance of the processor used for computations. On the other hand, to estimate the mean duration of the useful signal needed to successfully acquire one satellite at a given C/N_0, statistical simulations are processed. Indeed, it has been shown that the output of the acquisition loop presented in Figure 1 is :

$$T = \sum_{k=1}^{M} \left| s_4^i(k) \right|^2$$

s_4^i follows a normal distribution, with non zero mean and variance $\sigma_{n_4^i}^2$. As a consequence, $\sum_{k=1}^{M} \left(s_4^i / \sigma_{n_4^i} \right)^2$ is a new statistic which follows a non-central Chi-square distribution, with M degrees of freedom. The non-centrality parameter λ is defined as the sum of the squared mean of the normal distribution s_4^i :

$$\lambda = \sum_{k=1}^{M} E\left[\frac{s_4^i(k)}{\sigma_{n_4^i}^2} \right]^2$$

$$= MT_p \cdot \frac{C}{N_0} \cdot \left(\frac{\sin\left(\pi \Delta f_d^i \cdot T_p\right)}{\pi \Delta f_d^i \cdot T_p} \right)^2 \cdot \sum_{k=1}^{M} K_c^2(k)$$

where :

– C is the power of the signal at the output of the antenna.

Given the statistic of the output of the acquisition loop, it is then possible to simulate the entire acquisition process by generating directly the output T. Consequently, to estimate the performance in terms of required signal duration, the output of the acquisition loop is generated

randomly, according to the number of non-coherent and coherent integration as well as the C/N_0 of the signal to acquire and the Doppler residual. Once the criterion is obtained, the detection process based on a maximum peak detection is engaged. If the detection fails, the dwell time is increased until the peak detection succeeds. For each C/N_0, the acquisition procedure is repeated 10000 times to compute the statistic of the required signal duration Probability Density Function, as well as its Cumulative Density Function. Simulations are run for a static user and typical C/N_0s encountered indoors. In the following, C/N_0s values have to be understood as C/N_0s at the output of the quantifier stage, which is the last filter of the RF front-end part.

IV – ACQUISITION TIME

Since the handled device is likely to be used by a pedestrian moving in urban areas, the A-GPS receiver is likely to acquire weak signals. On the other hand, the position computation process shall be fast enough for an easy use. The trade-off between time to successfully acquire and sensitivity becomes an issue. Taking advantage of the assistance data and according the methodology presented in the previous section, the following then focuses on the performance of the acquisition process in terms of required signal duration and processing time.

a) Required signal duration

As an illustration of the acquisition procedure, a typical PDF and its corresponding CDF representation are plotted in Figure 7 and in Figure 8 respectively. Contrary to the PDF presented in [Basti04], the shape is not constituted of plateaus, but it is rather bell shaped, which is consistent with our acquisition strategy.

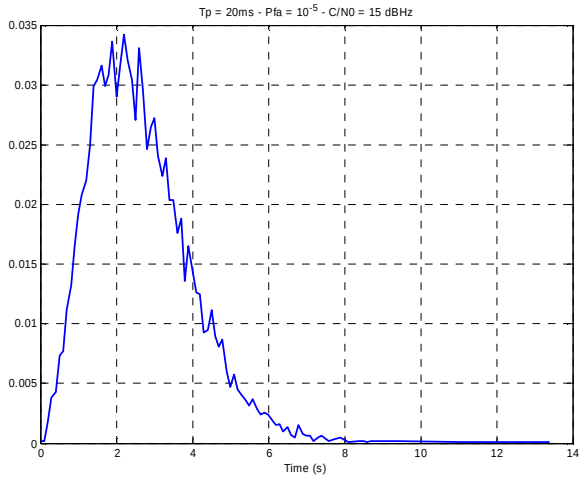

Figure 7 – Required signal duration PDF. C/N_0 = 15 dBHz.

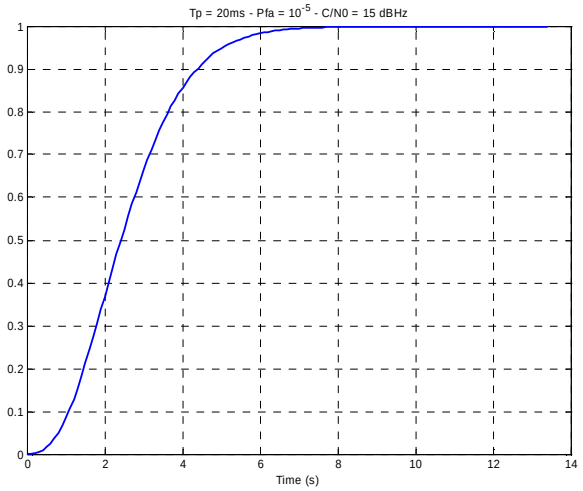

Figure 8 – Required signal duration CDF. C/N_0 = 15 dBHz.

Indeed, in the classical serial dwell search studied in [Basti04], a dwell time is fixed and then used to explore all the bins from the acquisition uncertainty region. In our case, the entire uncertainty region is explored at once to detect a correlation peak, based on a maximum detection process. If the detection fails, the number of non coherent integrations, and consequently the dwell time, increases until successful acquisition.

As a comparison, different PDFs are plotted in Figure 9 for a false alarm probability of 10^{-5} and a C/N_0 of 19 dBHz. As it can be expected, the larger the coherent integration time, the lower the time needed to acquire. Indeed, assistance data provide mean to reduce the overall number of Doppler bins, even if large coherent integration time are used.

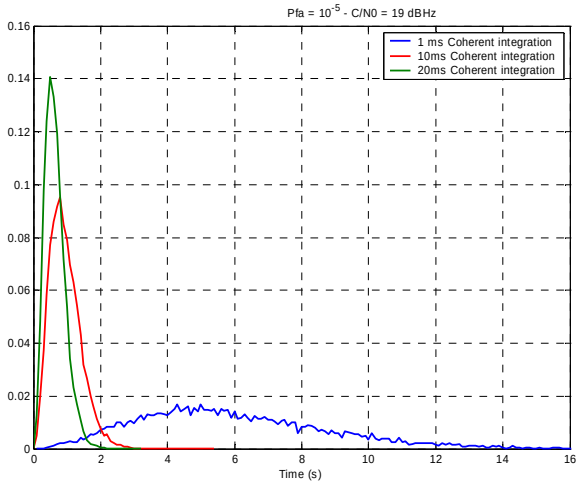

Figure 9 – Required signal duration PDF for three coherent integration times.

Then for each C/N_0, the mean required signal duration is

computed from the corresponding Probability Density Functions previously obtained. The duration estimation is computed based on the following formula :

$$\overline{T}_{C/N_0} = \sum_{t=0}^{t_{end}} t \cdot f_{C/N_0}(t)$$

where :

- f is the PDF obtained by simulation for a given C/N_0, P_{fa} and coherent integration time.
- t_{end} is the time span on which the PDF is defined.

Results on the mean duration of signal required to proceed a successful acquisition are plotted in Figure 10 for three different coherent integration times of 1ms, 10ms and 20ms. As expected, the higher the coherent integration number, the lower the length of signal that has to be processed. Values are very small, compared to the classical ones obtained using the basic Holmes formula dedicated to single dwell serial search strategy. This tends to prove that the FFT acquisition strategy based on a maximum detection test is much more efficient.

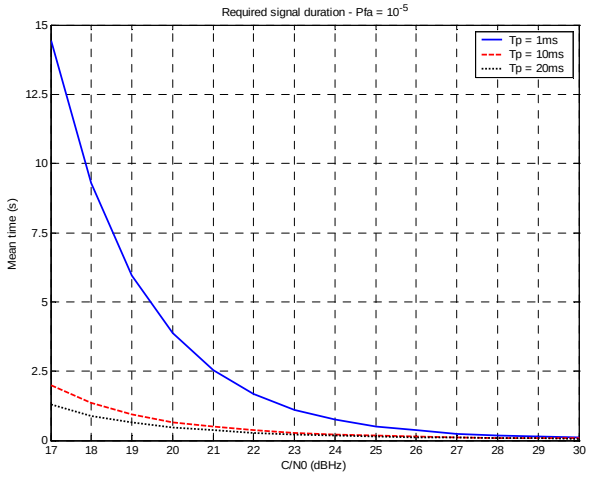

Figure 10 – Mean signal duration for successful acquisition.

However, even if the estimation of the signal length needed to acquire the corresponding satellite is known, this is only one part of the overall time to proceed. Since the acquisition process and then position computation is software implemented, one has to take into account the computational time. This is studied in the next subsection.

b) Processing time

The processing time is estimated using two different chipsets. In the following, the two Digital Signal Processors TMS320C55x and TMS320C64x from Texas Instruments are considered. The TMS320C55x is the digital signal processing core of the TI OMAP1510 dual core microprocessor platform. The basic characteristics of the DPSs are given in Table 3.

DSP	*TMS320C55x*	*TMS320C64x*
Frequency (Mhz)	144 to 200	300 to 1000
MIPS	288 to 400	2400 to 8000

Table 3 – DSP performance.

The estimation of the processing time needed to acquire one satellite is based on the path the signal follows through the acquisition structure presented in Figure 1. The time needed to the RF front-end to process the data collection is in the following omitted, as well as the one for base-band transformation. Indeed, both are fixed times, independent of the power of the signals to acquire. The different stages to be taken into account in the processing time computation are :

1. The Doppler removal.
2. The FFT correlations.
3. The square and sum operations.
4. The search of the maximum peak.

Performance of both DSPs was found on the Texas Instrument's website, using available benchmarks. Results presented in Berkeley Design Technology Inc's reports such as [BDTI04] and [BDTI02] were also used to assess the DSPs performance. The basic operations computed when the signal goes through the acquisition structure are listed in Table 4.

Operations	Elapsed time (cycle)	
	TMS320C55x	*TMS320C64x*
Complex FFT	4786	1243
Maximum search value	134	74
Maximum index search	256	122
Matrix (16×16) multiply	2720	1611

Table 4 – Typical cycles per instruction for a 256-point vector.

The TMS320C64x has also dedicated functions such as the sum-and-square or the autocorrelation ones that do not perform the TMS320C55x. These functions were taken into account during the TMS320C64x simulations. Moreover, since no precise information was available to determine accurately the number of processor cycles needed for memory readings and writings, a 20 % penalty factor of the total processing time was taken into account and added to the final result.

TMS320C55x test results

The first test was conducted using the characteristics of a

TMS320C55x DSP with a clock speed of 168MHz. In Figure 11 is plotted the final mean acquisition time taking into account both the signal duration and the processing time, for three typical coherent integration times. For light indoor environment, where the C/N_0s are typically between 20dBHz and 30dBHz, the overall time needed to successfully acquire one satellite is well below 5 seconds for large coherent integration times, and less than 8 seconds for the other case. Obviously, the lower the C/N_0s, the greater the time to successfully acquire one signal.

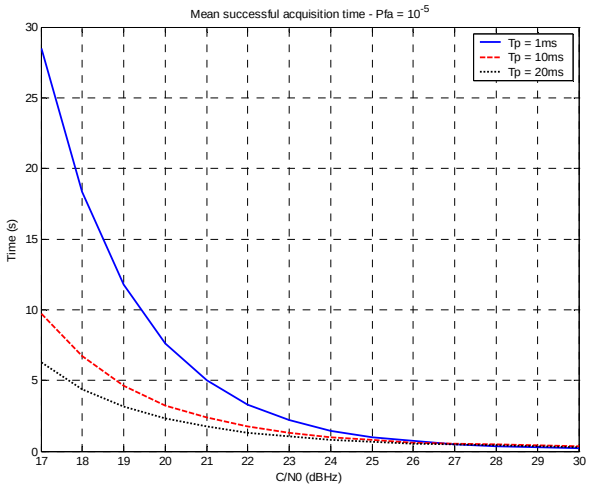

Figure 11 – Overall mean acquisition time.

The contribution of the different stages on the overall acquisition time is plotted in Figure 12 for typical indoor signals. It is shown that the greatest contribution in the 1ms coherent integration case comes from the signal collection. The FFT correlation processing is the second greatest contribution. The others are negligible compared to the two previous ones.

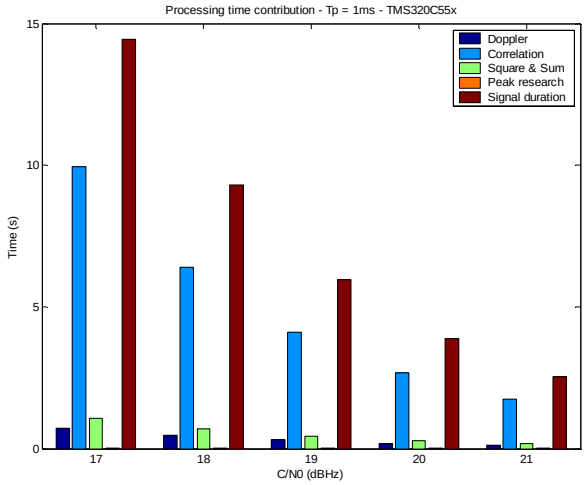

Figure 12 – Contributions of the different stages for a coherent integration time of 1ms.

In Figure 13, the same contributions are plotted, but with a large coherent integration time. In that case, the stage having the greatest contribution is the correlation one.

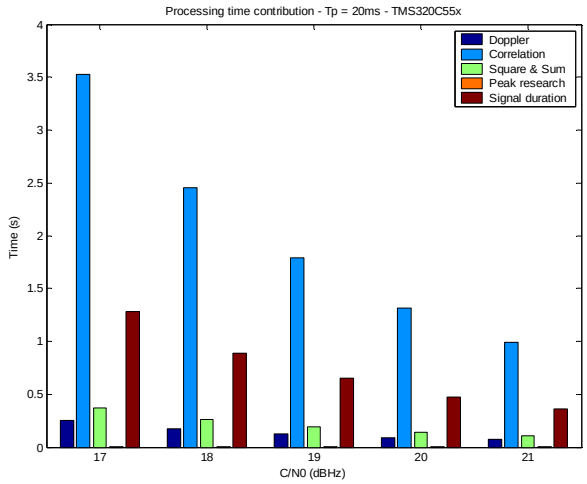

Figure 13 – Contributions of the different stages for a coherent integration time of 20ms.

TMS320C64x test results

DSPs are likely to improve their performance in a near future. Referring to the architecture of the OMAP1510, it can be foreseen that in the next few years, more powerful chipsets will be embedded in handheld devices. Therefore, results involving a new generation of DSP are presented. The DSP chosen is the TMS320C64x with a clock speed of 1GHz.

The overall mean acquisition time needed to acquire one satellite is plotted Figure 14. Compared to the previous results with the TMS320C55x, performance is improved, with a well reduced mean successful acquisition time, especially in the case of weak signals acquisition.

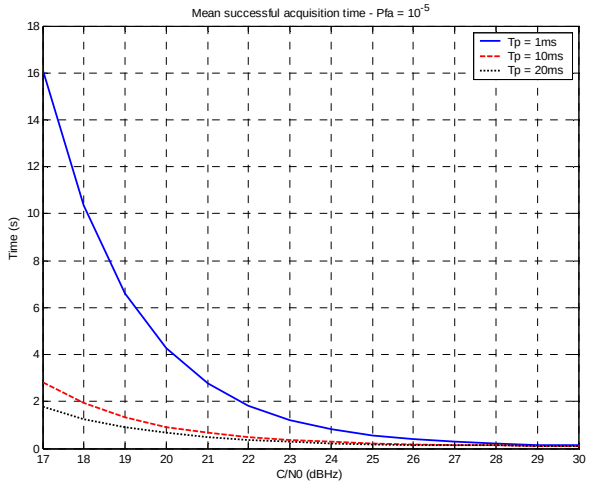

Figure 14 – Overall mean acquisition time.

The contribution of the different stages is plotted as well in Figure 15 and Figure 16. Whatever the coherent integration time, the main contribution on the overall successful acquisition time is the signal collection.

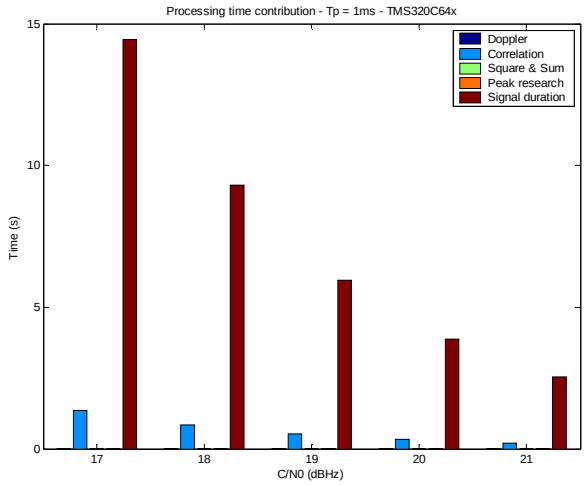

Figure 15 – Contribution of the different stages for a coherent integration time of 1ms.

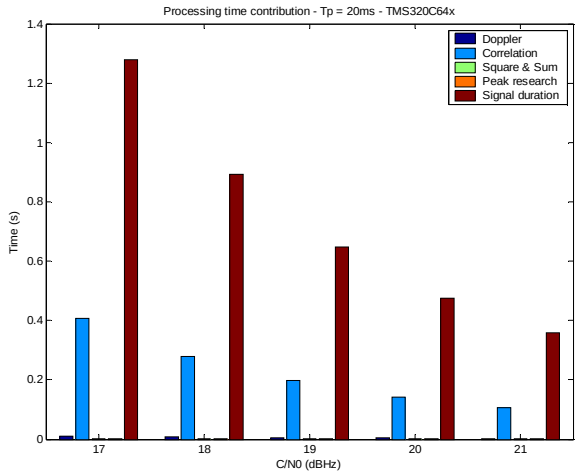

Figure 16 – Contribution of the different stages for a coherent integration time of 20ms.

c) Processing time correlation comparison

The TMS320C64x has a dedicated autocorrelation function, whose performance in terms of cycles needed to execute the instruction is given in benchmarks. It is then possible to compare the efficiency of both correlation techniques, the temporal one and the FFT one.

Results are presented in Figure 17. The worst case of a short coherent integration time was chosen in the simulation. The improvement of the correlation stage using FFTs is obvious, especially for weak signals with C/N_0s below 20dBHz. This makes the FFT correlation the most powerful technique that should be used in software receivers, especially if the signals to acquire are weak.

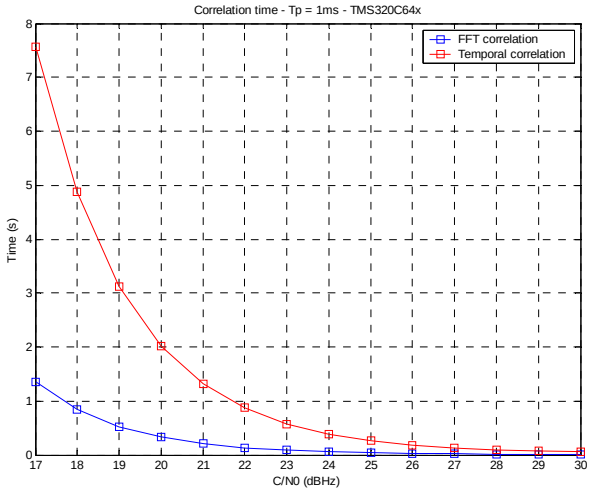

Figure 17 – FFT and temporal correlation processing performance.

CONCLUSION

In this paper, a precise software-based A-GPS acquisition using FFT correlations has been studied. Simulations were conducted to analyse the performance of such a structure in terms of mean time to successfully acquire one satellite. After having derivated the expression of the signal at the output of the acquisition loop, statistical processes were used to simulate the acquisition process. Based on the acquisition strategy and correlation peak detection method, the PDF of the mean time needed to acquire one satellite was computed, for different C/N_0s. It has been shown that the mean duration of the signal required to perform a successful acquisition was less than 2.5s for large coherent integration times (10ms to 20ms), but about 14s for short coherent integration times (typically 1ms), for C/N_0s higher than 17 dBHz.

Moreover, a focus was put on the processing time. For the TMS320C55x DSP, the processing time can not be neglected compared to the required signal duration needed to perform a successful acquisition. For the new generation DSP TMS320C64x, the time needed to process the data can be neglected only for short coherent integration times and light indoor signals (C/N_0s higher than 20 dBHz).

FFT correlations and classical temporal ones have also been compared for the TMS320C64x DSP. It has been shown that the FFT correlation is the best choice in terms of time to process, especially for weak signals below 20 dBHz, and consequently is well suited for software-based acquisitions.

In this paper, only static acquisition was studied. Obviously, the contribution to the overall Doppler induced by the motion of the user will increase the number of Doppler bins and as a consequence the processing time.

Alcatel Space has implemented such an acquisition technique on an OMAP1510 platform, as shown in Figure 18. Test campaign is currently in progress. Nevertheless, first results in light indoor environments corroborate the estimated times needed to successfully acquire GPS signals.

Figure 18 – OMAP1510 platform.

REFERENCES

[Basti04] – Bastide F. (2004). *Galileo E5a/E5b and GPS L5 Acquisition Time Statistical Characterization and Application to Civil Aviation*. ION GNSS 2004.

[BDTI02] – BDTI. (2002). *Inside the LSI Logic ZSP500*.

[BDTI04] – BDTI. (2004). *A BDTI analysis of the Texas Instrument TMS320C64x*.

[Digge01] – Diggelen F., Abraham C. (2001). *Indoor GPS Technology,* Global Locate, Inc. CTIA Wireless-Agenda, Dallas.

[Navst95] – *GPS Standard Positioning Service Signal Specification*. 2nd edition, June 1995.